Journal of
Nanoscience and Nanotechnology
Vol. 8, 1–5, 2008

Large Scale Preparation of β-$AgVO_3$ Nanowires Using A Novel Sonochemical Route

Changjie Mao, Xingcai Wu, and Jun-Jie Zhu*

Key Lab of Analytical Chemistry for Life Science (MOE), School of Chemistry and Chemical Engineering, Nanjing University, Nanjing 210093, P. R. China

A large number of β-$AgVO_3$ nanowires with diameter of 30–60 nm, and length of 1.5–3 μm have been successfully synthesized by a simple and facile low-temperature sonochemical route. The morphologies and structures of the nanowires were characterized by X-ray powder diffraction (XRD), X-ray photoelectron spectroscopy (XPS), transmission electron microscopy (TEM), scanning transmission electron microscopy (SEM), and thermal gravimetric analysis (TGA). Cyclic voltammetry and charge–discharge experiments were applied to characterize the electrochemical properties of the nanowires as cathode materials for lithium-ion batteries. In the initial discharge and charge process, the as-prepared $AgVO_3$ nanowires showed the initial charge and discharge capacities of 69 and 102 (mAh)/g, respectively. It is anticipated that the β-$AgVO_3$ nanostructures are promising cathode candidates in the application of primary lithium-ion batteries.

Keywords: β-$AgVO_3$ Nanowires, Sonochemical Route, Cyclic Voltammetry, Charge–Discharge Measurement.

RESEARCH ARTICLE

1. INTRODUCTION

One-dimensional (1D) nanostructured materials have attracted much attention due to their distinctive geometries, novel physical and chemical properties, and potential application in numerous areas such as single electron transistors,[1] field effect transistors,[2] interconnections in nanoelectronics,[3] lasers,[4] photodetectors,[5–7] and sensors.[8–10] Therefore, there are a number of methods for the preparation of 1D nanomaterials[11–16] (i.e., template method, chemical vapor deposition and hydrothermal method, etc.). In recent years, sonochemical method[17,18] is a fast-growing area in the preparation of nanomaterials. The chemical effects of ultrasound arise from acoustic cavitation, that is, the formation, growth, and implosive collapse of bubbles in a liquid. When solutions are exposed to high-intensive ultrasound irradiation, bubbles in the solution are implosively collapsed by acoustic fields can produces intense local temperatures (>5000 K), high pressures (>20 MPa), extremely rapid cooling rates (>10^{10} K/s),[19] thus sonochemical method can drive many chemical reaction. Ultrasound irradiation offers an attractive method for the preparation of nanosized materials and has shown rapid growth in its application to materials science because of its unique reaction effects.

It is well known that the silver vanadium oxide compounds (AgVO) are both important as catalysts and cathode materials.[20] Among them, $AgVO_3$ is the typical silver vanadium oxide compounds. Over the past years, there have been some reports on the synthesis of $AgVO_3$ nanomaterials.[21–24] However, to develop simple, fast and low-cost synthesis methods for the control over the morphology of $AgVO_3$ is of great importance for broadening and improving their industrial applications. Herein, we report a facile and fast sonochemical route for the preparation of β-$AgVO_3$ nanowires, which requires neither sophisticated techniques nor catalysts.

2. EXPERIMENTAL DETAILS

2.1. Synthesis

All the reagents used were of analytical purity and were used without further purification. In a typical procedure, a mixture of 2.5 mmol vanadium pentoxide powders, 5 mmol silver nitrate and 2.5 mmol 1,6-hexanediamine (as a organic template) was dissolved in 50 mL distilled water in an 100 mL round-bottom flask. Then this solution mixture was exposed to high-intensity ultrasound irradiation under ambient air for 60 min. Ultrasound irradiation was accomplished with high-intensity ultrasonic probe (Xinzhi Co., Xinzhi, China; 1.0 cm-diameter; Ti-horn, 20 KHz, 100 W/cm^2) immersed directly in the reaction solution.

*Author to whom correspondence should be addressed.

The sonication was conducted without cooling. When the reaction was finished, a brown precipitate was obtained. After cooling the sample to room temperature, the precipitate was separated by centrifuging at a rotation rate of 9000 rpm. It was then washed with distilled water and absolute ethanol in sequence, and dried in air at room temperature. The final product was in the form of dark brown powders and was characterized by XRD, XPS, SEM, TEM, and TGA.

2.2. Characterization

Powder X-ray diffraction (XRD) was conducted on a Philip X'pert X-ray diffractometer with Cu Kα radiation ($\lambda = 1.5418$ Å). X-ray photoelectron spectra (XPS) were recorded on an ESCALAB MK II X-ray photoelectron spectrometer, using nonmonochromatized Mg Kα X-ray as the excitation source and choosing C1s (284.6 eV) as the reference line. The TEM images were taken on a JEOL JEM-200CX transmission electron microscope, using an accelerating voltage of 200 kV. SEM images were taken by a LEO-1530VP scanning electron microscope, using an accelerating voltage of 200 kV.

2.3. Electrochemical Properties

Electrochemical measurements were carried out using two-electrode cells with lithium metal as the counter electrode. The working electrodes were fabricated by compressing the mixture of 80 wt% active materials, 10 wt% acetylene black, and 10 wt% ploytetrafluoroethylene (PTFE) onto an aluminum foil. The cell assembly was operated in an Ar-filled Labconco glovebox. The electrolyte solution was 1 M $LiPF_6$ dissolved in a mixture of ethylene carbonate (EC), dimethyl carbonate (DMC), and diethyl carbonate (DEC) with the volume ratio of EC:DMC:DEC = 1:1:1. Discharge–charge curves were recorded from 3.5 to 1 V at a constant current density of 125 mA/g using a roofer battery tester (Shenzhen, China) at room temperature.

3. RESULTS AND DISCUSSION

The XRD pattern of the as-synthesized $AgVO_3$ nanowires is shown in Figure 1. All diffraction peaks can be perfectly indexed to the monoclinic system with the lattice constants $a = 17.87$, $b = 3.58$, $c = 8.036$ Å, and $\beta = 101.33°$, which are in good agreement with the literature [JCPDS card 29-1154]. No peaks of any other phases were detected, indicating the high purity of the product. The XRD patterns indicated that relatively lower-crystallized $AgVO_3$ crystals could be easily obtained under the current synthetic conditions.

XPS measurements provided further information for the evaluation of the composition and purity of the product. The wide-scan XPS spectrum of the as-prepared product

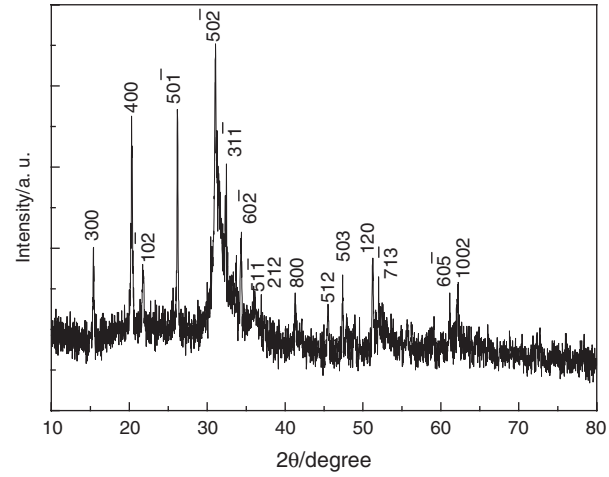

Fig. 1. Powder XRD pattern of the as-prepared $AgVO_3$ nanowires.

is shown in Figure 2(a). The binding energy was calibrated using the C 1s energy of 284.6 eV. No peaks of other elements except C, O, Ag, and V were observed in the spectrum, indicating the high purity of this product. Parts *b*, *c* and *d* of Figure 2 show the high-resolution XPS spectra of Ag(3d), V(2p) and O(1s), respectively. The two strong peaks at the Ag region of 380.6 and 386.6 eV were respectively assigned to Ag 3d (5/2) and Ag3d (3/2), whereas the two peaks located at 529.2 eV and 536.2 eV corresponded to V 2p (3/2) and V 2p (1/2) respectively. The other peak located at 542.4 eV was attributed to O 1s. The atomic ratio of the Ag:V:O in $AgVO_3$ calculated from the peak area was approximately 1:1:3, which was consistent with the given formula for $AgVO_3$ within the experimental errors.

The morphologies of the final samples were examined by scanning electron microscopy (SEM) and transmission electron microscopy (TEM). It can be observed that the product represents a wire-like morphology (Fig. 3(a)). A representative TEM image (Fig. 3(a)) and SEM image of the as-prepared samples (Fig. 3(b)) reveal that this sample is composed of a large quantity of nanowires with the diameter in the range from 30 to 60 nm, and the length is about 1.5–3 μm. The TEM image (Fig. 3(a)) and SEM image (Fig. 3(c)) indicate the presences of a few Ag particles on the surfaces of the nanowires, which is due to the loss of silver during the sample preparation.[25]

The influence of reaction conditions, such as, temperature, reaction time, and organic template, on the morphology has been investigated. A series of experiments showed that the short reaction times resulted in impurity phase due to incomplete reaction. The reaction temperature was also found to be a key factor for the formation of $AgVO_3$ nanocrystals. When hydrothermal temperature was lower than 60 °C, $AgVO_3$ nanocrystals could not be formed. It may be that the V_2O_5 was stable enough at this temperature, so that it did not hydrolyze to $AgVO_3$ nanocrystals. When temperature was controlled in the

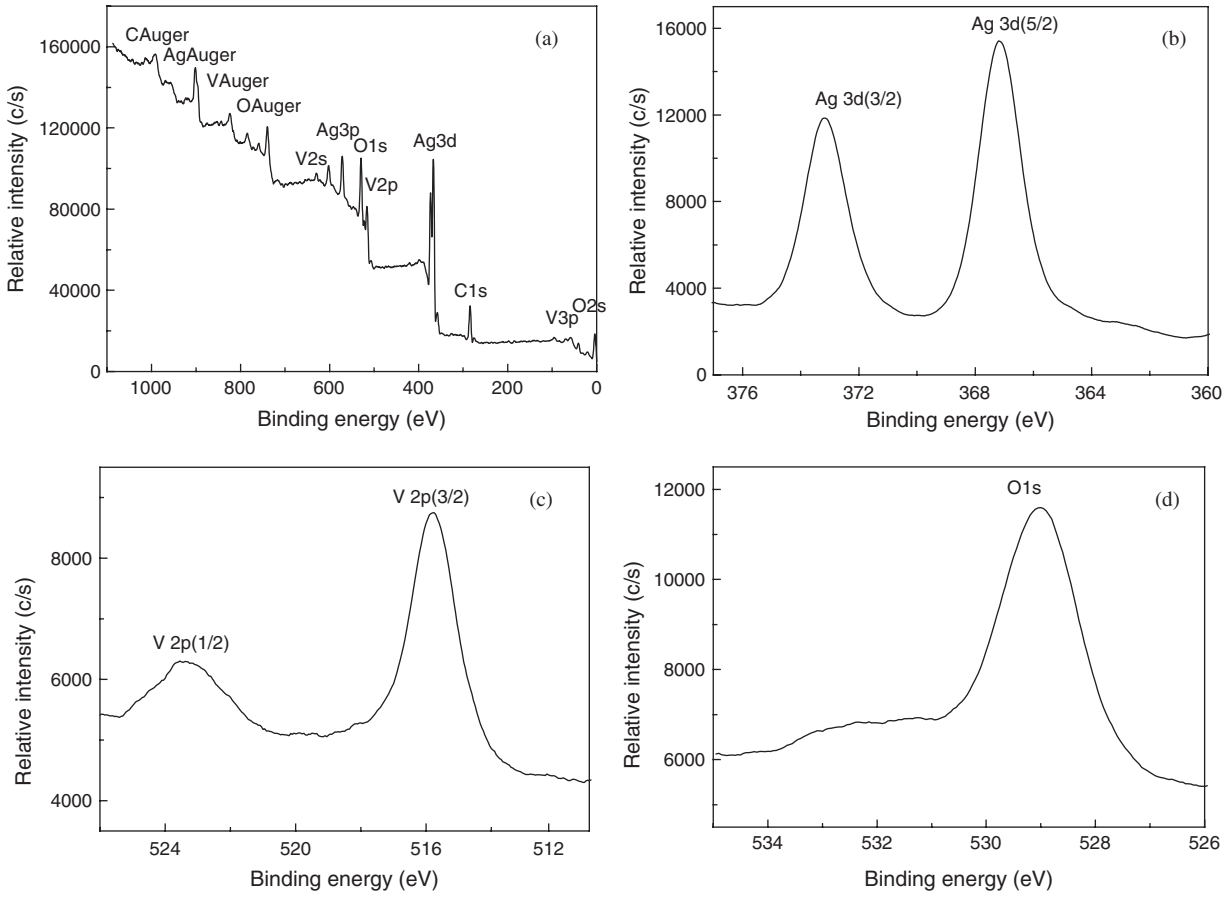

Fig. 2. XPS spectra of the as-prepared $AgVO_3$ nanowires. (a) Wide scan spectrum. (b) High-resolution spectrum for Ag (3d). (c) High-resolution spectrum for O (1s). (d) High-resolution spectrum for V (2p).

range of 70–170 °C, the morphology was the mixture of nanoparticles and nanobelts. It may be that reaction rate became slow at low temperature. Without the addition of organic template (1,6-hexanediamine), the morphology was the mixture of nanoparticles and nanorods. Hence, 1,6-hexanediamine played an important role in the morphological control of $AgVO_3$ nanocrystals, which could be ascribed to the fact that 1,6-hexanediamine could enhance the dissolution and reaction.

Yu group[26] performed some research on the possible growing mechanism of $Na_2V_6O_{16} \cdot 3H_2O$ nanobelts. There are some similarities in our system to their studies. Therefore, we believe that when temperature increased, the formed complex of Ag^+ and 1,6-hexanediamine might be decomposed, and bulky vanadium pentoxide was dissolved and polymerized under low alkali conditions to form VO_3^- ions. When the reaction proceeded to a certain extent, these species and silver ions formed $AgVO_3$. The whole reaction process can be expressed as follows:

$$\text{Ag-1,6-hexanediamine}^+ = \text{Ag}^+ + \text{1,6-hexanediamine}$$

$$V_2O_5 + OH^- = VO_3^- + H_2O$$

$$VO_3^- + Ag^+ = AgVO_3$$

The thermal stability of the $AgVO_3$ nanowires was studied by thermal gravity analysis in flowing N_2 atmosphere. The thermal gravity curve (Fig. 4) shows weight lost between 37° and 700°, which corresponds to the decomposition of residual organic templates and the loss of water between vanadium oxide layers respectively.

Figure 5 displays the initial discharge–charge curve and the corresponding incremental capacity plot for $AgVO_3$ nanowires. It exhibits two successive cathodic peaks characterized by lithium ion insertion process and an anodic peak corresponding to lithium ion extraction process in the incremental capacity plots. In the cathodic polarization process, three characteristic peaks were observed at around 2.11, 1.86, 1.12 V versus Li^+/Li, corresponding to complicated multistep electrochemical lithium intercalation processes; while in the following anodic polarization, one peak was located at 3.02 V, corresponding to the lithium extraction processes. However, the peak shape of $AgVO_3$ nanowires obviously became broader, possibly due to its relatively lower crystalline nature as indicated in its XRD pattern. On the other hand, two well-defined potential plateaus for discharging and a potential plateaus for charging are also observed, which is in well accordance with the results in the corresponding incremental capacity

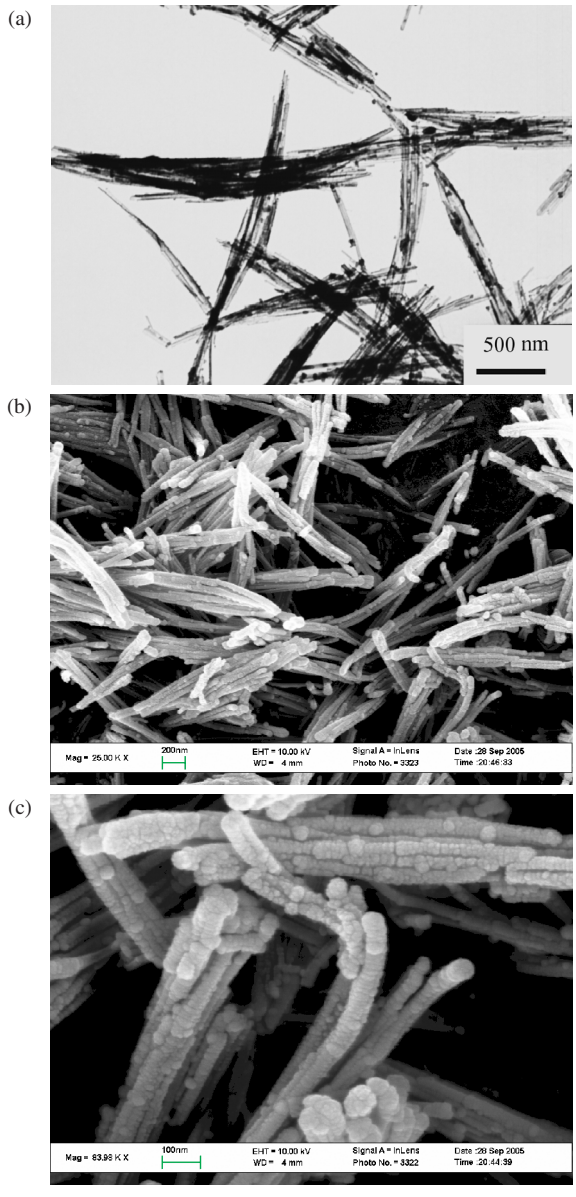

Fig. 3. Morphologies of as-prepared $AgVO_3$ nanowires. (a) A typical TEM image; (b) a typical SEM image; (c) a higher magnification SEM image.

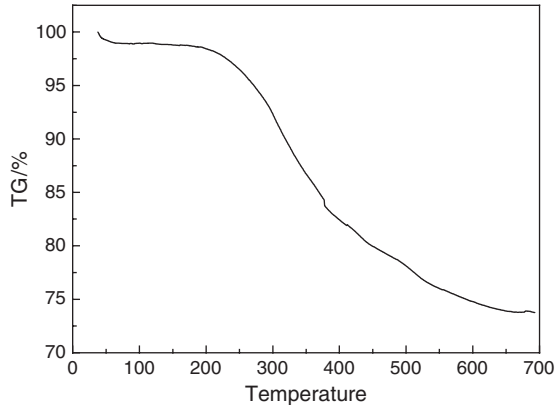

Fig. 4. TGA curve of as-prepared $AgVO_3$ nanowires.

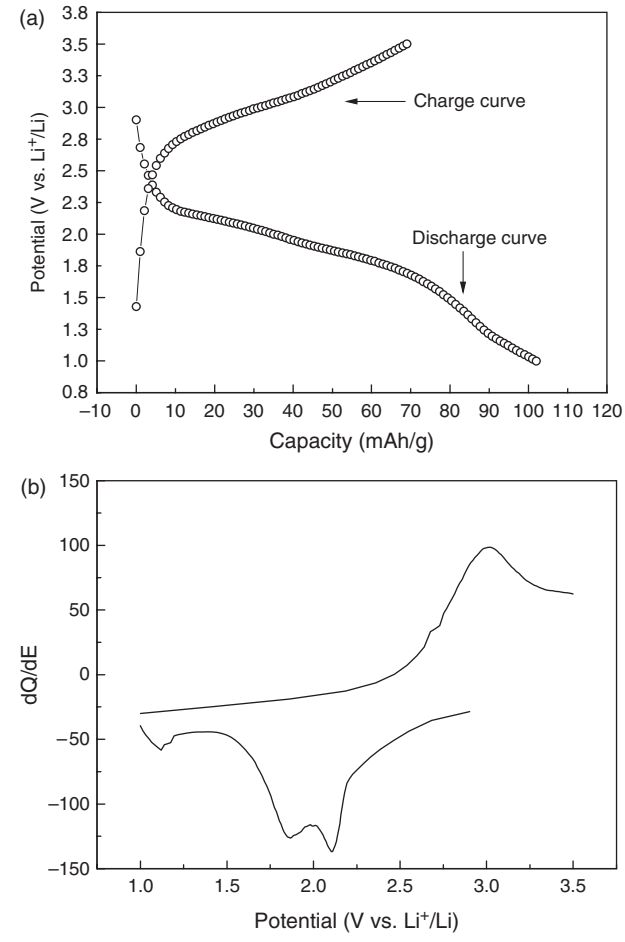

Fig. 5. The initial discharge–charge curves (a) and the corresponding incremental capacity plots (b) for $AgVO_3$ nanowires cycled at 125 mA/g between voltage limits of 1 and 3.5 V.

plots. The initial discharge 102 mAh/g and charge capacity (69 mAh/g) of $AgVO_3$ nanowires were significantly lower, which can be ascribed to higher electrode/electrolyte contact area and shorter path lengths for electronic and lithium ion transport.

4. CONCLUSION

In summary, a novel sonochemical route has been used to prepare $AgVO_3$ nanowires with diameter of 30–60 nm, and length of 1.5–3 μm. Cyclic voltammetry and charge–discharge experiments were applied to characterize the electrochemical properties of the nanowires as cathode materials for lithium-ion batteries. The as-prepared $AgVO_3$ nanowires showed the initial charge and discharge capacities of 102 and 69 (mAh)/g, respectively.

Acknowledgments: This work was financially supported by the National Natural Science Foundation of China (Nos. 20635020, 90606016, 20671050), Jiangsu Scientific foundation (BK2006114) and China Scholarship

Council (No. 20062027). Authors also thank the help from Professor Jinghong Li of Tsinghua University.

References and Notes

1. S. J. Tans, M. H. Devoret, H. Dai, A. Thess, R. E. Smalley, L. J. Geerligs, and C. Dekker, *Nature* 386, 474 **(1997)**.
2. R. Martel, T. Schmidt, H. R. Shea, T. Hertel, and P. Avouris, *Appl. Phys. Lett.* 73, 2447 **(1998)**.
3. A. M. Morales and C. M. Lieber, *Science* 279, 208 **(1998)**.
4. X. F. Duan, Y. Huang, R. Agarwal, and C. M. Lieber, *Nature* 421, 241 **(2003)**.
5. J. Wang, M. S. Gudiksen, X. Duan, Y. Cui, and C. M. Lieber, *Science* 293, 1455 **(2001)**.
6. H. Kind, H. Yan, B. Messer, M. Law, and P. Yang, *Adv. Mater.* 14, 158 **(2002)**.
7. D. Zhang, C. Li, S. Han, X. Liu, T. Tang, W. Jin, and C. Zhou, *Appl. Phys. A: Mater. Sci. Process.* 76, 163 **(2003)**.
8. J. Kong, N. R. Franklin, C. Zhou, M. G. Chapline, S. Peng, K. J. Cho, and H. Dai, *Science* 287, 622 **(2000)**.
9. C. Li, D. Zhang, X. Liu, S. Han, T. Tang, J. Han, and C. Zhou, *Appl. Phys. Lett.* 82, 1613 **(2003)**.
10. Y. Cui, Q. Wei, H. Park, and C. M. Lieber, *Science* 293, 1289 **(2001)**.
11. D. W. Yan and C. R. Wang, *J. Nanosci. Nanotechnol.* 7, 2487 **(2007)**.
12. M. K. Govind, V. K. Paliwal, A. G. Vedeshwar, and S. M. Shivaprasad, *J. Nanosci. Nanotechnol.* 7, 1841 **(2007)**.
13. D. Vrbanic, A. Meden, B. Novosel, S. Pejovnik, P. Umek, M. Ponikvar, and D. Mihailovic, *J. Nanosci. Nanotechnol.* 7, 982 **(2007)**.
14. W. Q. Yang, L. Dai, L. P. You, B. R. Zhang, B. Shen, and G. G. Qin, *J. Nanosci. Nanotechnol.* 6, 3780 **(2006)**.
15. P. Mohanty, J. Park, G. Lee, and B. Kim, *J. Nanosci. Nanotechnol.* 6, 3376 **(2006)**.
16. L. Berti, A. Alessandrini, C. Menozzi, and P. Facci, *J. Nanosci. Nanotechnol.* 6, 2382 **(2006)**.
17. S. X. Lu, K. Sivakumar, and B. Panchapakesan, *J. Nanosci. Nanotechnol.* 7, 2473 **(2007)**.
18. L. P. Jiang, S. Xu, J. J. Miao, H. Wang, and J. J. Zhu, *J. Nanosci. Nanotechnol.* 6, 2584 **(2006)**.
19. K. S. Suslick, S. B. Choe, A. A. Cichowlas, and M. W. Grinstaff, *Nature* 353, 414 **(1991)**.
20. K. J. Takeuchi, A. C. Marschilok, S. M. Davis, R. A. Leising, and E. S. Takeuchi, *Coordin. Chem. Rev.* 219, 283 **(2001)**.
21. Y. Liu, Y. G. Zhang, Y. H. Hu, and Y. T. Qian, *Chem. Lett.* 34, 146 **(2005)**.
22. J. G. Xie, X. Y. Cao, J. X. Li, H. Zhan, Y. Y. Xia, and Y. H. Zhou, *Ultra. Sonochem.* 12, 289 **(2005)**.
23. S. Sharma, M. PanthÖfer, M. Jansen, and A. Ramanan, *Mater. Chem. Phys.* 91, 257 **(2005)**.
24. S. Y. Zhang, W. Y. Li, C. S. Li, and J. Chen, *J. Phys. Chem. B* 110, 24855 **(2006)**.
25. H. W. Zandbergen, A. M. Crespi, P. M. Skarstad, and J. F. Vente, *J. Solid State Chem.* 110, 167 **(1994)**.
26. J. G. Yu, J. C. Yu, W. K. Ho, L. Wu, and X. C. Wang, *J. Am. Chem. Soc.* 126, 3422 **(2004)**.

Received: 18 January 2007. Accepted: 14 July 2007.